

Comparison of linear and non-linear blade model predictions in Bladed to measurement data from GE 6MW wind turbine

W Collier¹, J Milian Sanz²

¹DNV GL, One Linear Park, Avon Street, Bristol, BS2 0PS, UK

²GE Renewable Energy, Roc Boronat, 78, 08005 Barcelona, Spain

E-mail: william.collier@dnvgl.com jose-maria.milian-sanz@ge.com

Abstract: The length and flexibility of wind turbine blades are increasing over time. Typically, the dynamic response of the blades is analysed using linear models of blade deflection, enhanced by various ad-hoc non-linear correction models. For blades undergoing large deflections, the small deflection assumption inherent to linear models becomes less valid. It has previously been demonstrated that linear and non-linear blade models can show significantly different blade response, particularly for blade torsional deflection, leading to load prediction differences. There is a need to evaluate how load predictions from these two approaches compare to measurement data from the field.

In this paper, time domain simulations in turbulent wind are carried out using the aero-elastic code Bladed with linear and non-linear blade deflection models. The turbine blade load and deflection simulation results are compared to measurement data from an onshore prototype of the GE 6MW Haliade turbine, which features 73.5m long LM blades. Both linear and non-linear blade models show a good match to measurement turbine load and blade deflections. Only the blade loads differ significantly between the two models, with other turbine loads not strongly affected. The non-linear blade model gives a better match to the measured blade root flapwise damage equivalent load, suggesting that the flapwise dynamic behaviour is better captured by the non-linear blade model. Conversely, the linear blade model shows a better match to measurements in some areas such as blade edgewise damage equivalent load.

1. Introduction

Early research into the effect of geometrical non-linearity in rotating blades was conducted in the 1970s and 80s for the helicopter industry by Hodges [1] and for early large wind turbines by Friedmann [2]. Friedmann concluded that non-linear formulations were important to correctly capture aero-elasticity effects for large turbines.

The majority of early wind turbines had relatively stiff blades, and the effect of geometric non-linearity was small. Most turbines were therefore designed using linear models of blade deflection, which include an assumption of small deflections [3]. In the last 10 years, increasingly flexible blade designs have been developed and research has focused once more on geometric non-linearity. In 2004, Larsen [4] studied a multi-MW wind turbine and concluded that the change in effective rotor area due to blade model non-linearity was the key effect on steady state loads. In 2007/8, as part of the UPWIND project, Politis [5] and Riziotis [6] demonstrated the effect of blade model non-linearity on tip deflections in the flapwise and torsional directions on the NREL 5MW turbine [7]. The key design impact was a strong effect on blade root torsional fatigue loads. In 2011, Kallesoe [8] demonstrated the effect of non-linear models on edgewise-torsion coupling, importantly showing that the damping of edgewise modes can depend strongly on blade model non-linearity. In 2015, Manolas [9] also



identified strong influence of bending-torsion coupling and observed a shift in frequencies of the second edgewise mode when using a non-linear blade deflection model.

Recent work using Bladed [10] showed the strong effect on blade torsion from a non-linear model of blade deflection, and benchmarked the model against HAWC2 [11], which uses a similar multibody formulation to capture blade non-linearity.

There is a need to evaluate how load predictions from linear and non-linear blade deflection models compare to measurement data from the field. In this paper, time domain simulations in turbulent wind are carried out using the aero-elastic code Bladed (v4.7.0.83) using linear and non-linear blade deflection models. Power, load and blade deflection measurements were collected from an onshore prototype of GE 6MW Haliade turbine. Comparisons are conducted in three sections: power curve, load statistics and damage equivalent loads, and blade deflection in front of the tower.

It is noted that the presented results are only applicable to the studied turbine, and only serve to compare the linear and non-linear blade formulations within Bladed against the measured data.

2. Method

2.1. Simulation method

A non-linear blade deflection model can be defined in Bladed by splitting the blade into several linear bodies, as illustrated in Figure 1, for a two-part blade. As the outboard blade sections can undergo arbitrary large rotations, an accurate model of non-linear deflection is achieved when enough blade parts are used. The small deflection assumption is satisfied in each blade part.

The blade structural model within each blade part is based on Timoshenko beam elements and allows arbitrary orientation of the shear axis relative to the neutral axis [12]. Each body (e.g. a blade part) is an assembly of linear finite elements. The number of degrees of freedom is reduced by calculating Craig-Bampton modes [13] within each blade part. The linear model of each the blade part is enhanced by models of geometric stiffness based on work by Krenk [14].

The aerodynamic loads were calculated using blade element momentum theory, including models for dynamic stall, dynamic wake and a skew wake correction [12].

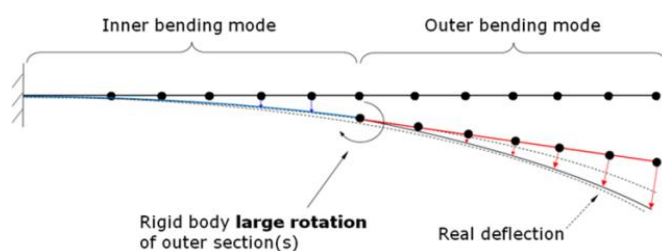


Figure 1: Non-linear “multi-part” blade model approach

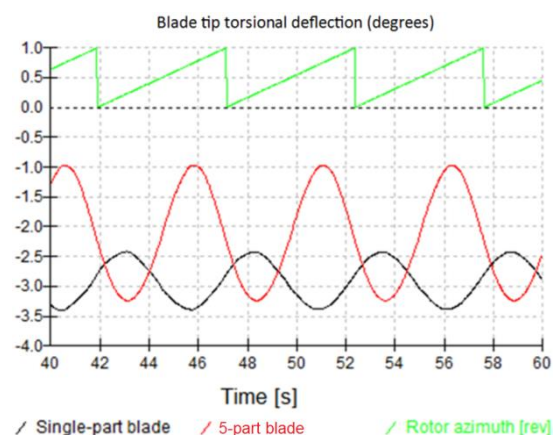


Figure 2: Tip torsional deflection with linear and multi-part blade models

A model of the onshore prototype of GE 6MW Haliade turbine was defined in Bladed 4.7.0.83, including a controller DLL that replicates the controller used on the turbine prototype. A linear blade model was defined by modelling the blade as a single finite element body. Enough linear blade modes were included to capture the first blade torsional mode. A multi-part model with 5 blade parts was also defined, with 8 modes on each part. To ensure model convergence, it was verified that a higher fidelity model with 9 blade parts gave very similar blade load and deflection results to the 5-part model. The single-part model included geometric stiffness terms to account for centrifugal stiffening, by capturing the effect of axial blade element loads on structural response. The multi-part model included a further geometric stiffness correction to include the effect of shear loads, to more accurately capture the blade torsional response.

The azimuthal variation in blade tip torsional deflection near rated wind speed with the linear and multi-part blade model is shown in Figure 2. The torsional deflection is calculated in Bladed by expressing the rotational deflection from the reference configuration as a pseudo-vector with three orthogonal components aligned with the blade root. The torsional deflection is taken to be the component of this vector parallel to the pitch axis. The torsional response of the blade to azimuthal load variation differs significantly in mean, amplitude and phase for the linear and multi-part blade models. This difference occurs because the multi-part blade model can more accurately calculate the internal torsional load along the blade, which has a significant component that is dependent on the deflection shape of the blade. Linear blade models don't account for the effect of blade deflection on the internal loads and dynamic response, as explained in [10]. This different torsional response is thought to be a key driver for differing blade load and deflections with linear and multi-part blade models.

2.2. Data collection method

An anemometer was used to measure wind speed, shear and turbulence intensity. The anemometer was located approximately 2 rotor diameters from the turbine. Measurement samples where the anemometer was in the turbine wake were excluded. Strain gauges were used to collect the measured load time histories at blade root, main shaft, and tower base. The tower base load location is located near the base of the turbine above the supporting jacket structure. Blade deflection near the tower was measured using a ground-based laser system.

2.3. Environmental conditions

Different environmental conditions were considered for the power curve, loads and blade deflection comparisons. For all comparisons the Kaimal turbulence model was used, with default parameters corresponding to IEC-61400-1 ed.3. The air density and wind shear were calculated for each wind speed bin and used in the simulations.

2.3.1. Power curve environmental conditions

10-minute Bladed simulations with turbulent wind were carried out between 5-15m/s wind speeds.

2.3.2. Loads comparison environmental conditions

10-minute Bladed simulations with turbulent wind were carried out at 6, 8, 10 and 12m/s wind speeds. Simulations were not performed above 12m/s due to lack of measurement data above this wind speed. The turbulence intensity chosen for the simulations was 11% and the measurement data was filtered for turbulence intensities close to this value.

The upflow angle was set to 0 degrees. Six turbulent seeds were used at each wind speed, considering two seeds at each yaw misalignment of 8, 0 and -8 degrees.

2.3.3. Blade deflection comparison environmental conditions

The wind speed and direction were matched exactly in simulation compared to measurement at the hub height. Three 10-minute time series were considered between 7.5 and 8.5 m/s. Blade deflection comparisons were considered at periods during which the wind turbine was not pitching and the operation variables (electrical power, generator torque and generator speed) matched well between simulations and measurements.

3. Results

In this section, comparison between simulated and measured turbine power curve, loads and blade deflections are presented. These simulations correspond to the three sets of environmental conditions listed above. Note that the y-axis in many plots is normalised or omitted to hide sensitive data.

3.1. Electrical Power

The comparison of mean electrical power of measurements and simulations is shown in Figure 3. It is observed that the match in mean power is good between measurement and simulation, with the difference generally less than 2%. The multi-part blade simulations predict slightly higher power.

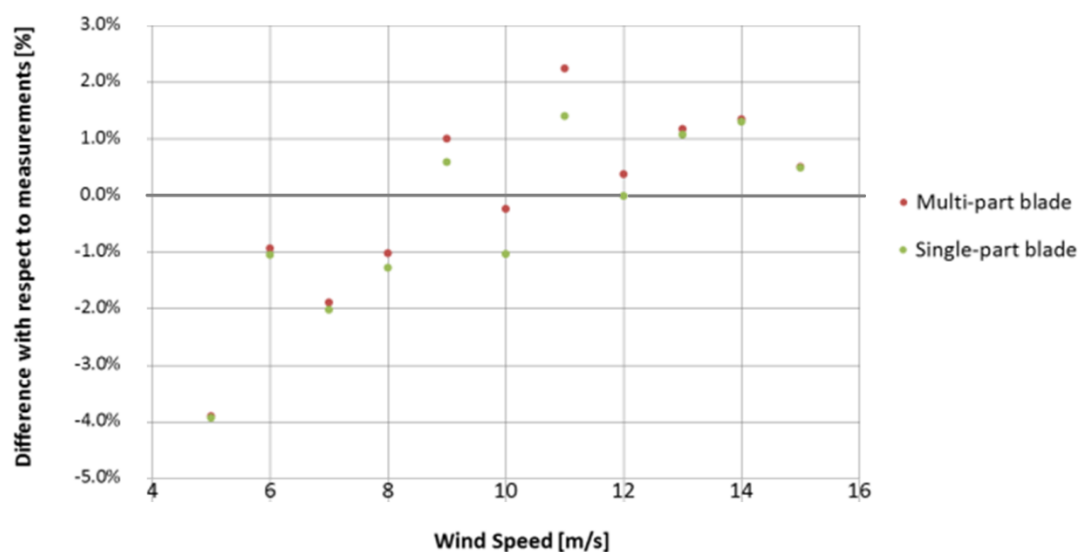


Figure 3: Electrical power measurements comparison with respect to measurements.

3.2. Loads

In this section, a match in turbine operating point between simulation and measurement is demonstrated by comparing main shaft torque and rotor speed.

Subsequently, blade, main shaft and tower loads are presented in detail. For each load variable the following is given: statistics (minimum, maximum, mean and standard deviation) and damage equivalent loads (DELs).

3.2.1. Operating point

Figure 4 and Figure 5 show a comparison of main shaft torque and rotor speed at the studied wind speeds. An excellent match in the mean values is observed, suggesting that the operating point is well matched for load comparisons.

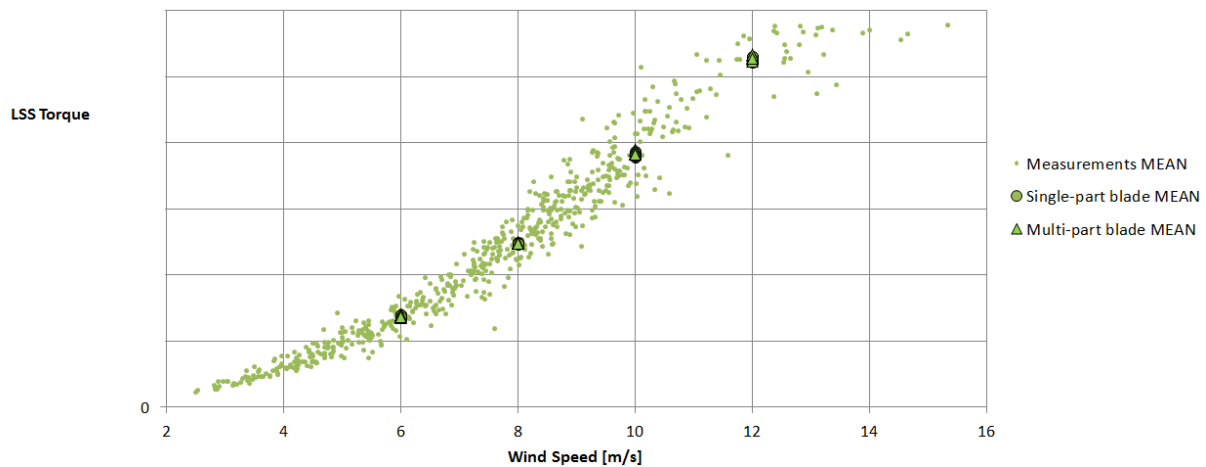


Figure 4: Mean values for main shaft torque

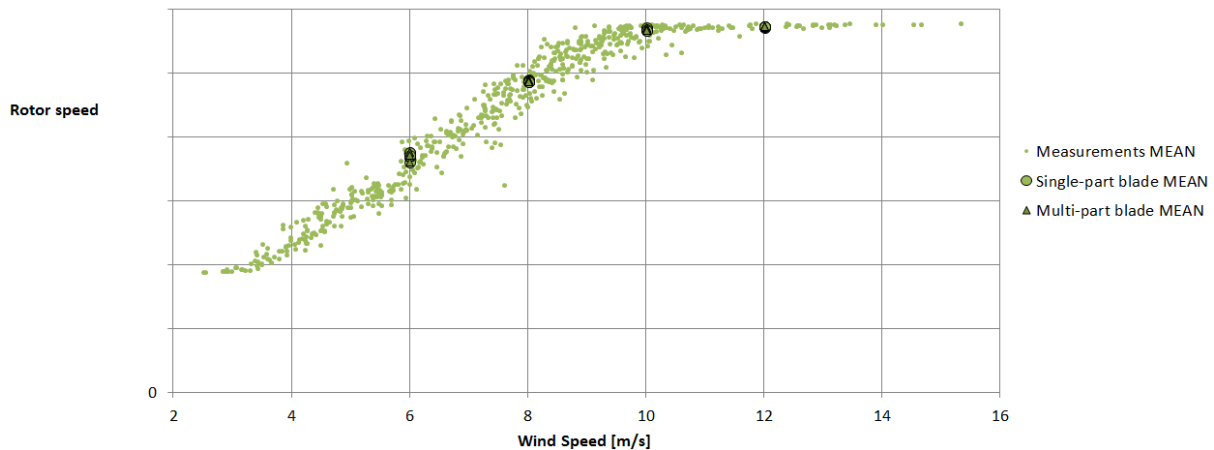


Figure 5: Mean values for rotor speed

3.2.2. Blade root flapwise moment

The statistics (min, mean, max and std. dev) of measured and simulated blade root flapwise bending moment are shown in Figure 6.

The single-part and multi-part simulations agree closely on mean blade root flapwise bending moment but are offset from the measured loads. The reasons for this offset are currently under investigation.

The single-part blade shows a better match on the maxima, but this is most likely due to the difference in the mean value present for single-part and multi-part blade.

The standard deviation plot shows that the simulated points with the multi-part blade are more centred in the cloud of points of the measured points. Results from simulations using the single-part blade are more conservative. This may suggest that the flapwise dynamic behaviour is captured more accurately with the multi-part blade model.

The damage equivalent loads for blade root flapwise bending moment are shown in Figure 7. The single-part and multi-part blade simulations show good match to measured DELs. As with the standard deviation results, the multi-part blade is closer to centre of cloud of measurements, and the single-part blade is slightly more conservative.

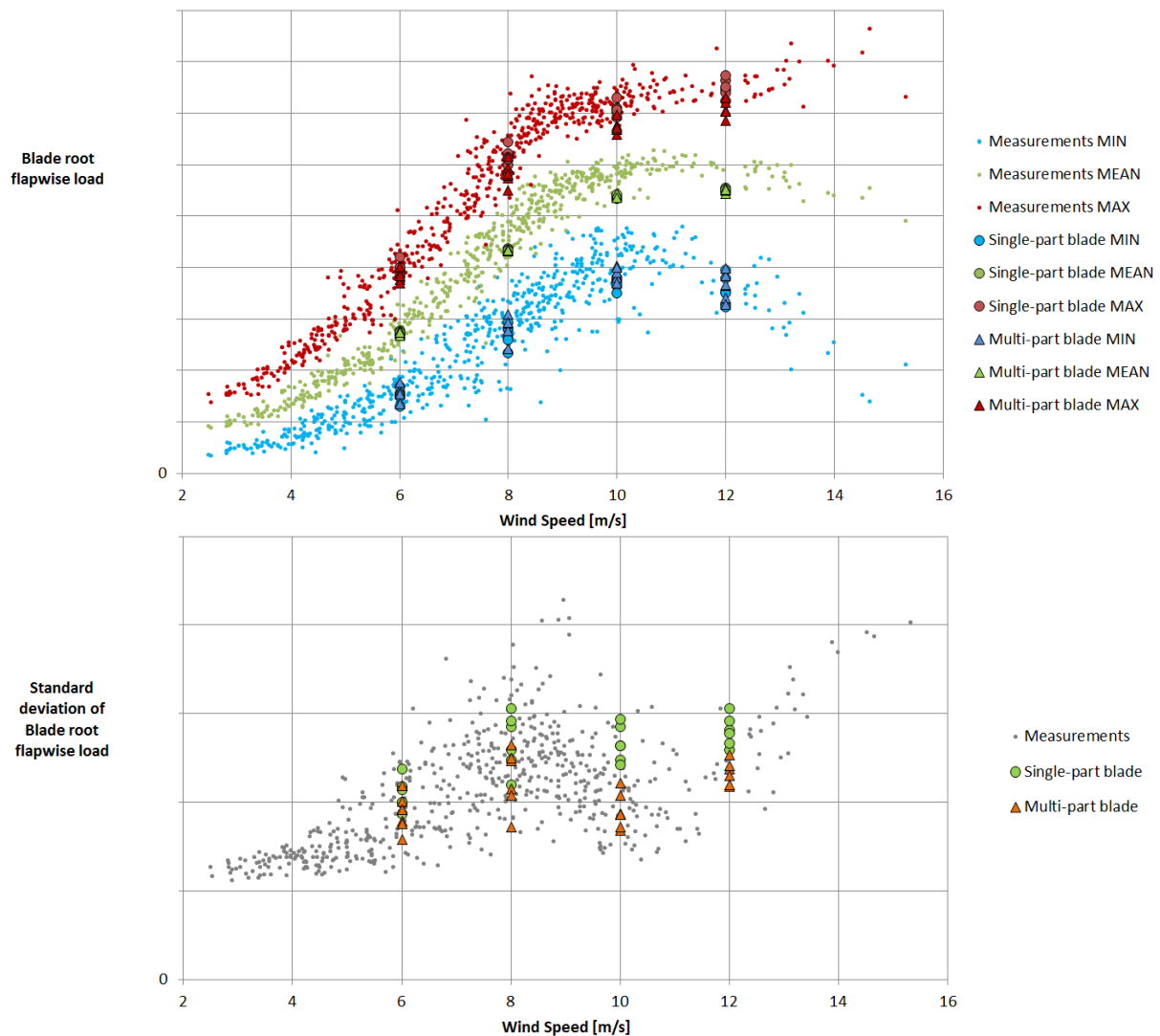


Figure 6: Load statistics for blade root flapwise bending moment

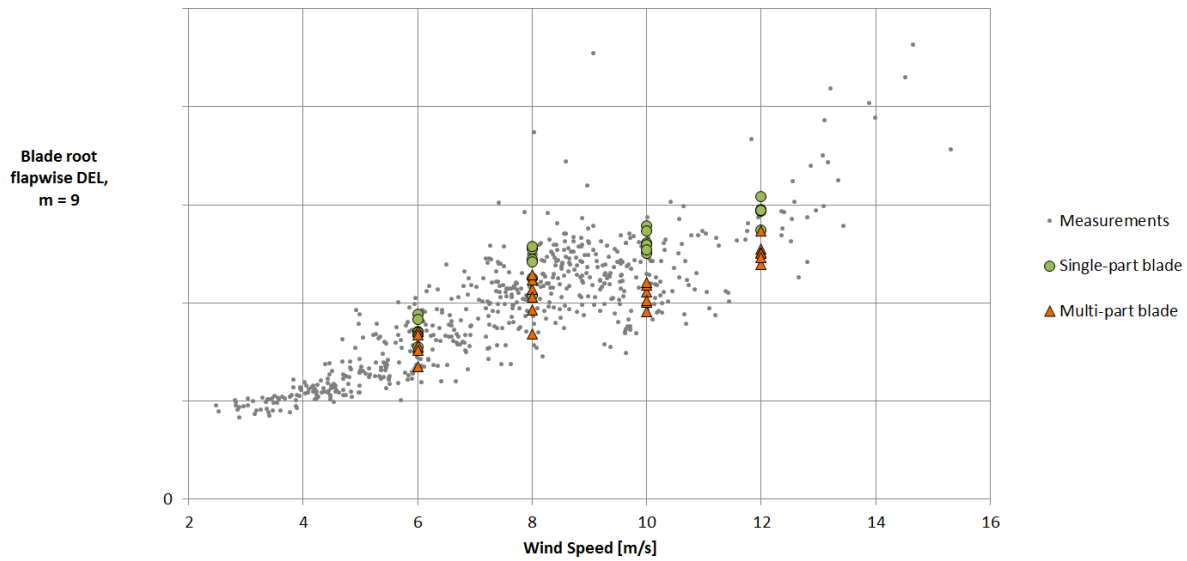


Figure 7: Damage equivalent loads for blade root flapwise bending moment

Power spectral density (PSD) analysis of a flapwise blade root load time history at 10m/s is shown in Figure 8. The presented measurement PSD was derived by averaging two PSDs corresponding to individual measured load time histories to reduce noise. These time histories had zero yaw error. The multi-part blade shows a better match to measurements at the 1p peak and in the troughs in between areas of high excitation. The measurements show more activity between the rotor speed multiples than in the simulations.

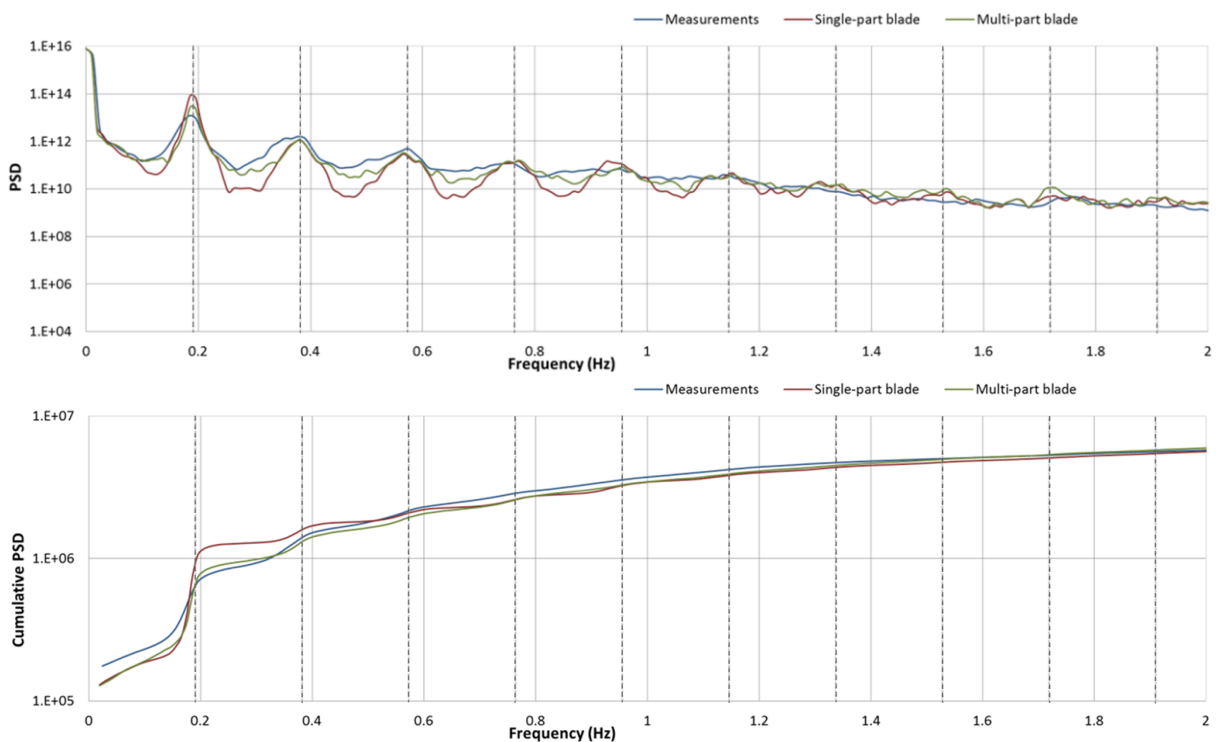


Figure 8: PSD of blade root flapwise bending moment at 10 m/s. Dotted points show multiples of rotor rotational frequency

Figure 9 shows a comparison of the periodic load components for both measurements and simulation, for 10m/s wind speed. This plot shows the average load at each azimuth angle for each 10-minute sample. The simulation shown has zero yaw error.

The multi-part blade is closer to measurements in terms of the amplitude of the signal, and the azimuth angles at which the maximum and minimum load occur. The position of the peaks is driven principally by the wind shear (which tends to give peaks near 0 and 180deg) and alternating gravity load that changes the blade torsion angle (this tends to give peaks near 90 and 270 deg). The combined effect of gravity loads and shear profile appears to be more accurately captured by the multi-part blade.

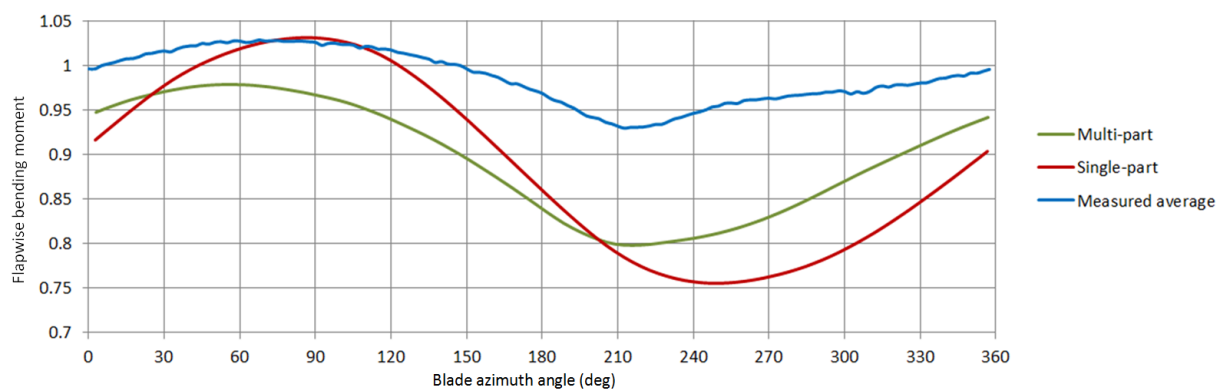


Figure 9: Periodic flapwise bending moment. 0 deg azimuth is the blade pointing upwards

3.2.3. Blade root edgewise bending moment

The statistics (min, mean, max) of measured and simulated blade root edgewise bending moment are shown in Figure 10. Generally the simulated loads match well with the measurements. The single-part blade shows a better match to the maxima.

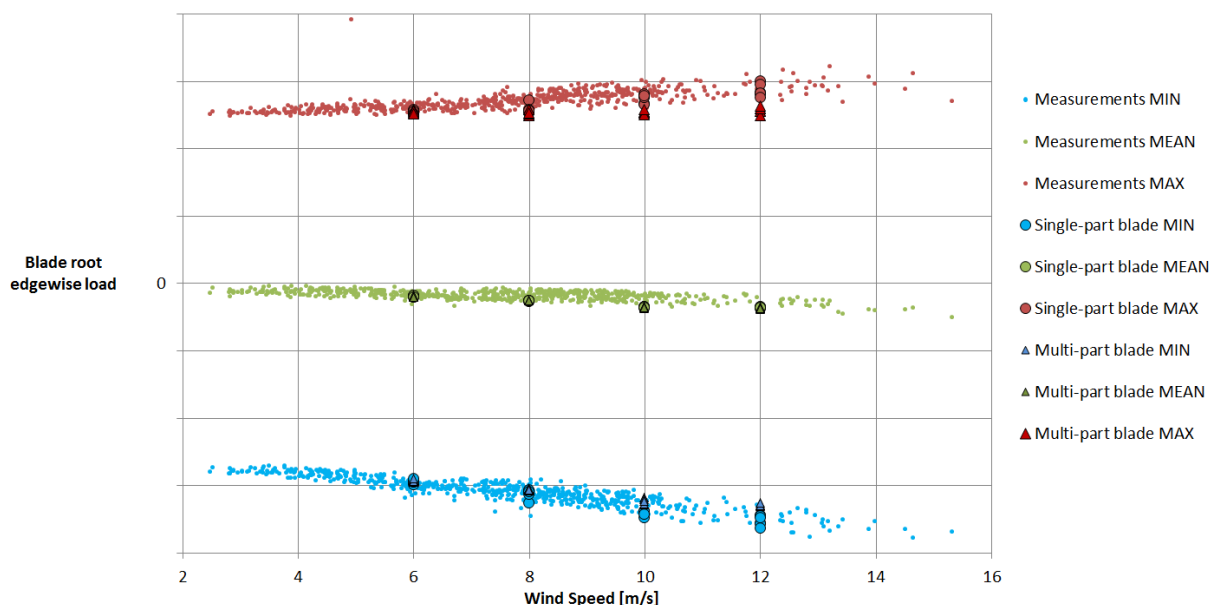


Figure 10: Load statistics for blade root edgewise bending moment

The damage equivalent loads for blade root edgewise loads are shown in Figure 11. Again the match between simulations and measurements is good, with single-part blade showing a slightly closer match to measurements.

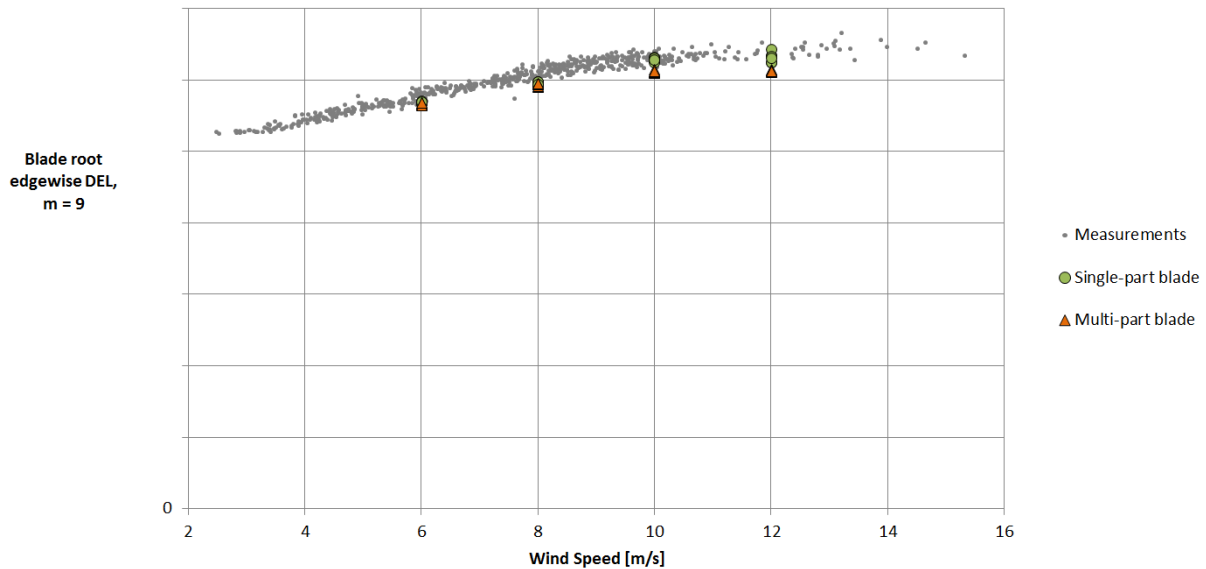


Figure 11: Damage equivalent loads for blade root edgewise bending moment

PSD analysis of the edgewise load history is shown in Figure 12.

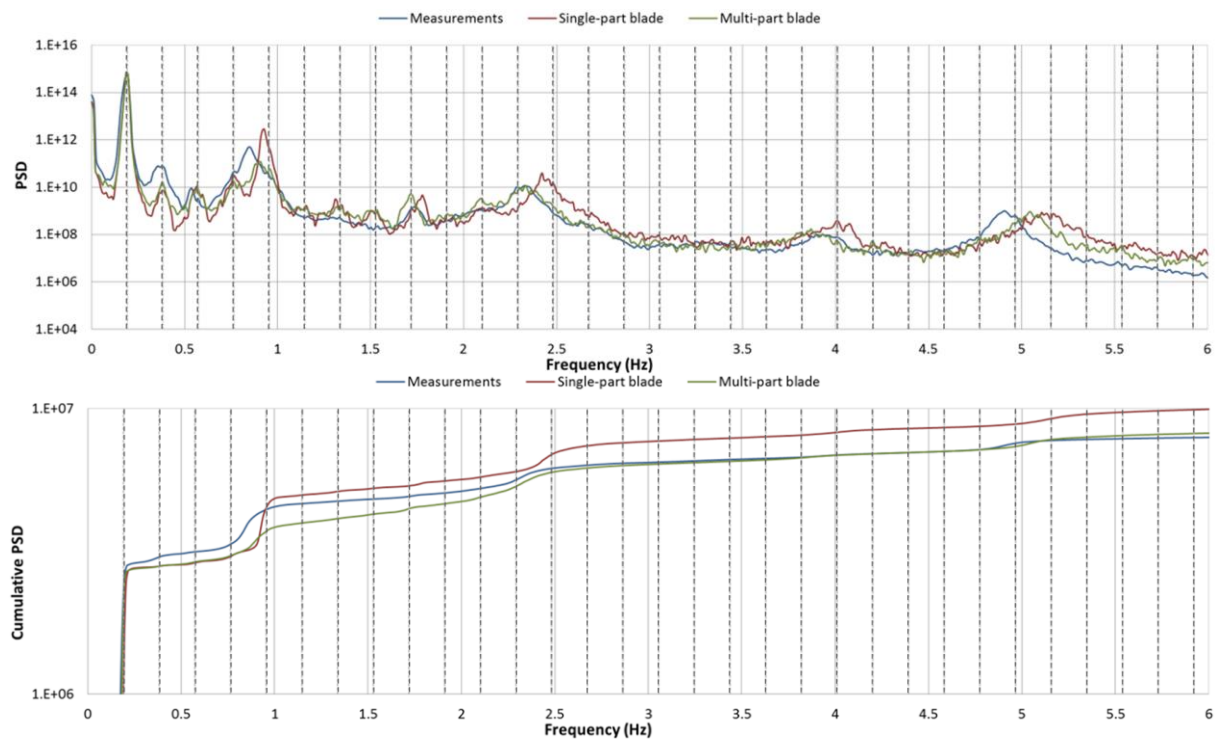


Figure 12: PSD of blade root edgewise moment at 10 m/s. Dotted lines show multiples of rotor rotational frequency

Both single-part and multi-part simulations show a very good match on the 1p peak; this is expected as this load is mostly driven by gravity. There is noticeable difference between simulations at

measurement at the 1st edgewise mode ($\sim 0.9\text{Hz}$). The higher activity at 1st edgewise frequency shows why the edgewise DELs are higher with the single-part blade approach. However, the cumulative PSD plot shows that the excitement of the first edgewise mode is better captured by multi-part blade than single-part blade. Analysis of linearised models in Bladed indicates a higher damping on the first edgewise rotor mode in the multi-part blade model than the single-part blade model, which may well account for the differing response of the first edgewise mode in the two models. This higher damping is likely a result of the more accurate bend-twist coupling captured in the multi-part blade model.

The multi-part blade results show a better match in frequency for the 2nd edgewise asymmetric mode at $\sim 2.35\text{Hz}$. This frequency difference occurs because the multi-part blade is able to account for the effect of structural deflection on blade vibrational frequency.

The better match in the PSD for multi-part blade to measurements is somewhat contradictory to the better match in DEL for single-part blade to measurements.

3.2.4. Main shaft torque DEL

Figure 13 shows the main shaft torque DEL comparison. Both the single-part and multi-part blade show a good match to measurements in terms of damage equivalent loads. At 6m/s, the simulated DELs are slightly lower than the measurements.

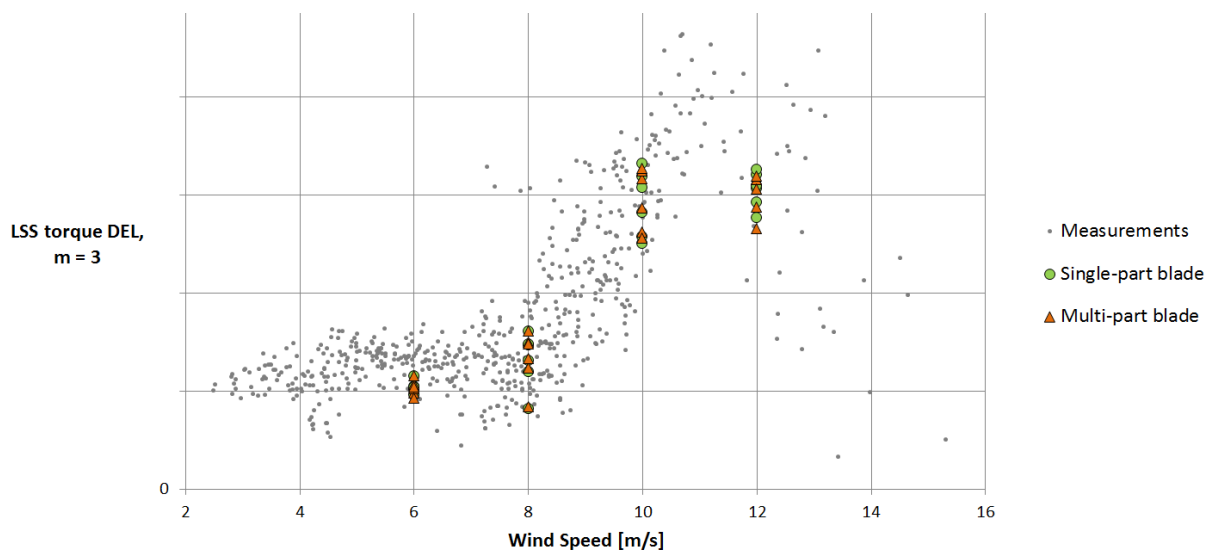


Figure 13: Damage equivalent loads for main shaft torque

3.2.5. Tower base overturning moment

The statistics (min, mean, max) of measured and simulated tower base overturning moment are shown in Figure 14. The single-part and multi-part blade show an excellent match in terms of statistics and damage equivalent loads.

Damage equivalent loads are shown in Figure 15. The single-part and multi-part blade both show a good match to measurements although the DELs are towards the bottom of the cloud of measurement values. It was found that the wind direction veer (which was not included in the presented simulations) is a possible explanation for this discrepancy, although this is still under investigation.

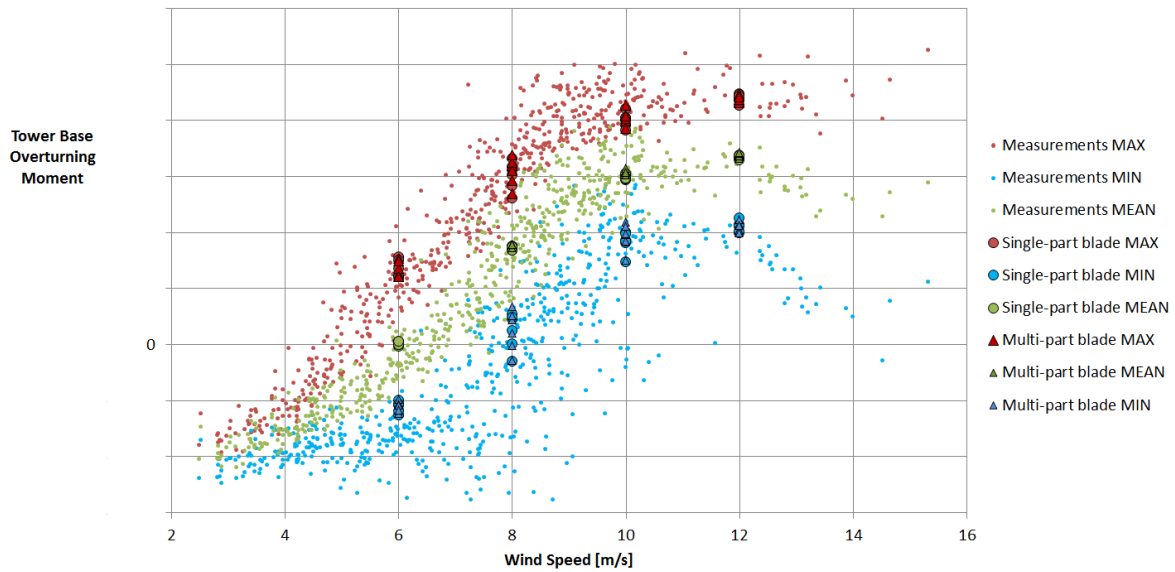


Figure 14: Load statistics for tower base overturning moment

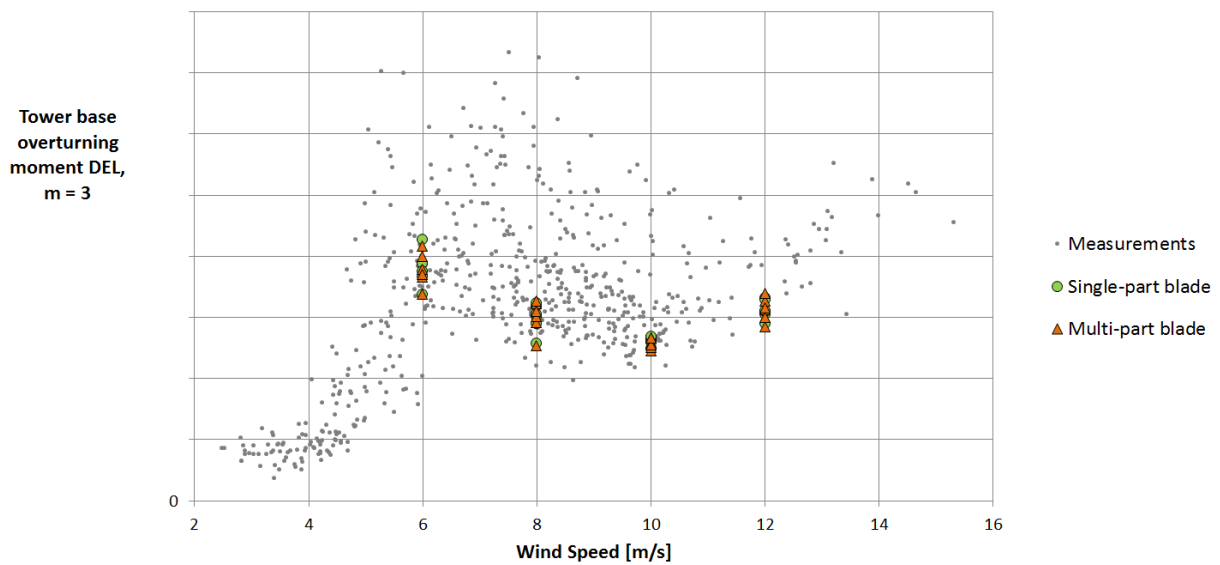


Figure 15: Damage equivalent loads for tower base overturning moment

3.3. Blade deflection in front of tower

As discussed in section 2.3.3. , the distance between the blade and the tower as it passes in front of the tower was measured using a ground-based laser system. The clearance was measured at a blade section 66m from the blade root. Approximately 7 minutes of time history from three samples were selected based on a good match in operating point between measurement and simulation. Simulated tower clearance was calculated through a combination of the static clearance and the blade deflection in front of the tower.

Figure 16 shows mean and minimum tower clearance from the time history samples. The results are normalised by the mean value of tower clearance measured. The single-part and multi-part blade simulations give similar results for the minimum and mean tower clearance. Mean values of simulated blade deflection show a good match to the measurements, with the simulation being slightly conservative (smaller tower clearance) in two of the three samples. The minimum tower clearance is smaller in the simulation compared to the measurement: the simulations are conservative compared to the measurements. A possible explanation for this discrepancy is that the wind conditions over the whole rotor were not well matched between measurement and simulation.

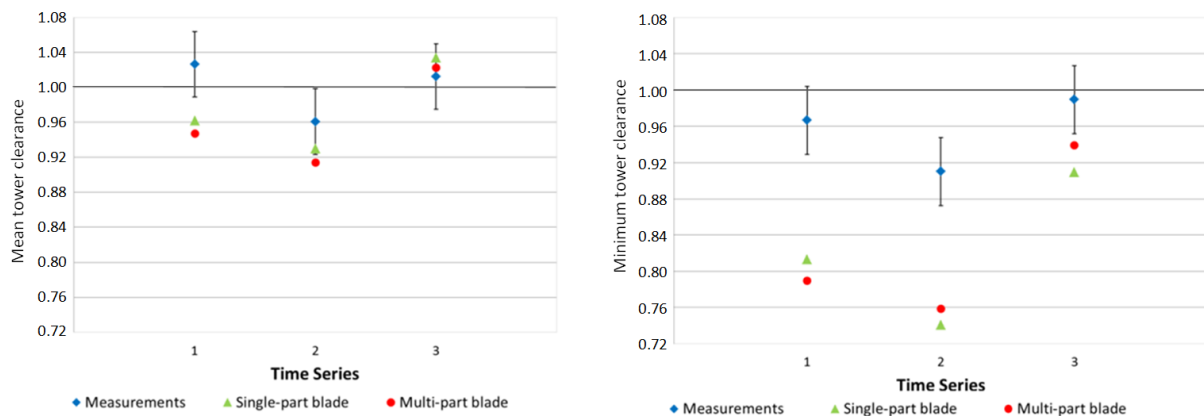


Figure 16: Tower Clearance Statistics comparison with respect to measurements.

4. Conclusions

Bladed 4.7 simulations using single-part and multi-part blade models both generally show a good match to the measurements from the Haliade 6MW onshore prototype in terms of electrical power, turbine loads and blade deflection.

The match in simulated and measured electrical power is very good. The measured power is generally within 2% of the simulated power.

For blade loads, a good match was found between measurement and simulation. Blade root flapwise DELs were more centred in the cloud of measured DELs for multi-part blade than for the single-part blade. Conversely, the single-part blade showed a better match to the edgewise blade loads. Both blade models can be considered as appropriate simulation approaches for this turbine based on these findings. A good match in main shaft torque and DELs was found between simulation and measurement, using both simulation models. Tower base overturning moment also showed an excellent match in terms of load statistics and DELs.

The mean value of tower clearance within the studied samples was found to match well between simulation and measurements, with no significant difference between the single-part and multi-part blade results. The minimum value of tower clearance was more conservative in the simulations than in the measurements.

References

1. Hodges D, Dowell E. “Non-linear equations of motion for the elastic bending and torsion of twisted non uniform rotor blades”. Technical Report TN D-7818, NASA, 1974.
2. Friedmann P. “Aero elastic stability and response analysis of large horizontal-axis wind turbines”. *Journal of Wind Engineering and Industrial Aerodynamics*. 1980; 5: 373401.
3. Hansen M, Sørensen J, Voutsinas S, Sørensen N, and Madsen H. “State of the Art in Wind Turbine Aerodynamics and Aeroelasticity” *Progress in Aerospace Sciences.*, 42, pp. 285–330, 2006
4. Larsen T, Hansen A, Buhl T. “Aeroelastic effects of large blade deflections for wind turbines” *Torque from Wind Conference*, 2004
5. Politis E, Riziotis V. “The Importance of Nonlinear Effects Identified by Aerodynamic and Aero-Elastic Simulations on the 5 MW Reference Wind Turbine,” UPWIND Project, Technical Report No. SES6. 2007
6. Riziotis A, Voutsinas S, Politis E, Chaviaropoulos P, Hansen A, Madsen H, Rasmussen F. “Identification of structural non-linearities due to large deflections on a 5MW wind turbine blade”. *EWEA Conference 2008*.
7. Jonkman J. NREL 5MW baseline wind turbine. Technical Report, NREL, Golden, Colorado, 2005.
8. B S Kallesoe. “Effect of steady deflections on the aero elastic stability of a turbine blade” *Wind Energy*. 2011: 14:209-224
9. Manolas D, Riziotis A, Voutsinas . “Assessing the Importance of Geometric Nonlinear Effects in the Prediction of Wind Turbine Blade Loads”. *ASME Journal Computational Nonlinear Dynamics* 10(4), 041008, 2015
10. Collier W, Bradstock P, Ravn M, Andersen C 2015. “Non-linear blade model in Bladed for prediction of deflection of large wind turbine blades, and comparison to HAWC2”. *EWEA Conference 2015*
11. Larsen T, Hansen A. “How 2 HAWC2, the user’s manual”
12. Garrad Hassan and Partners Ltd, *Bladed Theory Manual v4.7*, 2015
13. Craig, R. “Coupling of substructures for dynamic analyses: an overview”, *AIAA-2000-1573*
14. Krenk S. “Non-linear Modelling and Analysis of Solids and Structures”. Cambridge University Press 2009